1.A Direct-Drive, High-Gain, Hydrodynamics Equivalent Experiments Facility

Over the past several years the inertial confinement fusion (ICF) program has made significant progress in addressing a number of key physics issues. These advances have made it possible for the Department of Energy (DOE) to begin to address the requirements needed to achieve ICF's major objective—high gain in the laboratory. To date, a large effort has been devoted to the understanding, both experimentally and theoretically, of the national program's main approach to ICF—indirect drive.[1] However, recent achievements in directly driven capsule implosions[2,3] and the development and initial implementation of laser-beam-smoothing techniques[4–7] have shown that a direct-drive solution to the national program's goal, along with its potential savings in driver energy, deserves increased attention.

At present there are a number of key physics issues associated with high-gain, direct-drive pellet implosions for which little, if any, experimental data exists. This information is required by DOE to better determine the future role of direct drive. Here we present these physics issues as they pertain to a direct-drive, high-gain pellet implosion and discuss why a new direct-drive experimental facility is required to obtain this data base. Subsequent articles in this and the next LLE Review will present how this facility could be constructed as an upgrade to the present OMEGA laser facility, as well as preliminary design concepts of the implementation of many system features.

This article is divided into two sections: First, using a numerical simulation of a high-gain, direct-drive pellet implosion, the key physics issues, requiring increased experimental data, are presented. Second, the general requirements that a direct-drive facility will have to meet to carry out the relevant experiments are examined.

One-Dimensional, High-Gain, Direct-Drive Designs

Recently, several high-gain, direct-drive pellet designs, spanning an incident-energy range of 1.0 to 10.0 MJ, have been examined for both 351-nm and 270-nm illumination. They are all single-shell designs consisting of a low-atomic-number (Z) ablator surrounding a levitated cryogenic deuterium-tritium (DT) main fuel layer. The inner region of the pellet contains a DT-gas mixture whose density and composition are determined by the temperature of the main fuel layer. (Several designs were carried out with the main fuel composed of a DT/low-density CH foam mixture.[8] For this article, we limit discussion to pellet designs for which the main fuel layer is pure DT.)

The designs were carried out using the one-dimensional hydrodynamic code *LILAC*. *LILAC* contains Lagrangian hydrodynamics, tabular equation of state (SESAME),[9] thermonuclear

burn, multigroup particle transport, and multifrequency radiation transport. The opacities used in the multifrequency transport are obtained from reducing the Los Alamos National Laboratory (LANL), 2000-frequency-group, local thermodynamic equilibrium (LTE), Astrophysical Library[10] to a desired group structure (~ 50 groups are used for the simulations presented in this article). Laser-energy deposition is modeled by a geometric optics ray-trace algorithm[11] with energy deposited by inverse Bremsstrahlung along the ray path. Flux limitation of electron thermal transport[12] is incorporated as a "sharp cutoff" with the Spitzer-Härm electron thermal conductivity. [For the simulations presented in this article the value of the flux limiter f is set to 0.06 with the maximum permitted heat flux given by $q_{\max} = f\, n_e\, kT(kT/m_e)^{1/2}$. This value of f has been found to give the best numerical results of laser-energy absorption, x-ray conversion for moderate-Z materials, and hydrodynamic motion of recent OMEGA pellet implosions.[3,13]]

The first issue is to determine the effect of irradiation nonuniformity on direct-drive target implosions. Two-dimensional simulations of direct-drive pellet implosions show that illumination nonuniformities can adversely affect pellet implosion by two principal means. The first is development of long-wavelength ($\ell \leq 8$), secular (t^2) growth during the acceleration phase caused by variations in the drive pressure. The second is the seeding of short-wavelength modes that can then develop due to the Rayleigh-Taylor[14-16] instability at the ablation surface. Current two-dimensional simulations of high-gain, direct-drive pellet implosions indicate that illumination nonuniformities on target will have to be $\leq 1\%\ \sigma_{\text{rms}}$.[17]

Several investigators have examined the uniformity produced by overlapping multiple laser beams on spherical targets.[18-22] Research at LLE has emphasized the decomposition of the laser energy in terms of spherical harmonics to obtain information about the spatial wavelengths of the nonuniformity on target for a beam-overlap pattern.[22] The irradiation pattern on target can be expressed as the product of two factors: (1) a "single-beam" factor that depends on the focal position, f-number of the lens, assumed target conditions, energy and possible temporal imbalance between individual beams (power balance), and the individual beam profiles; and (2) a "geometric" factor that is determined by the number and orientation of the individual beams about the target.

Analysis of different beam configurations for given focus conditions and laser-beam profiles, has shown that increased uniformity can be obtained over a wider focal region by increasing the number of beams. Figure 38.3 shows the predicted rms illumination nonuniformity on target for 20, 32, 60, and 96 beams using an ideal quadratic radial-beam profile. All beam configurations provide adequate uniformity at a focus ratio of ~ 1 (tangential focus). However, during capsule implosion, the focus ratio shifts (toward the right along the abscissa in Fig. 38.3) because of the inward motion of the critical surface. Due to this motion, a system with significantly less than 60 beams, unlike the 60- and 96-beam configurations, fails to provide the required drive

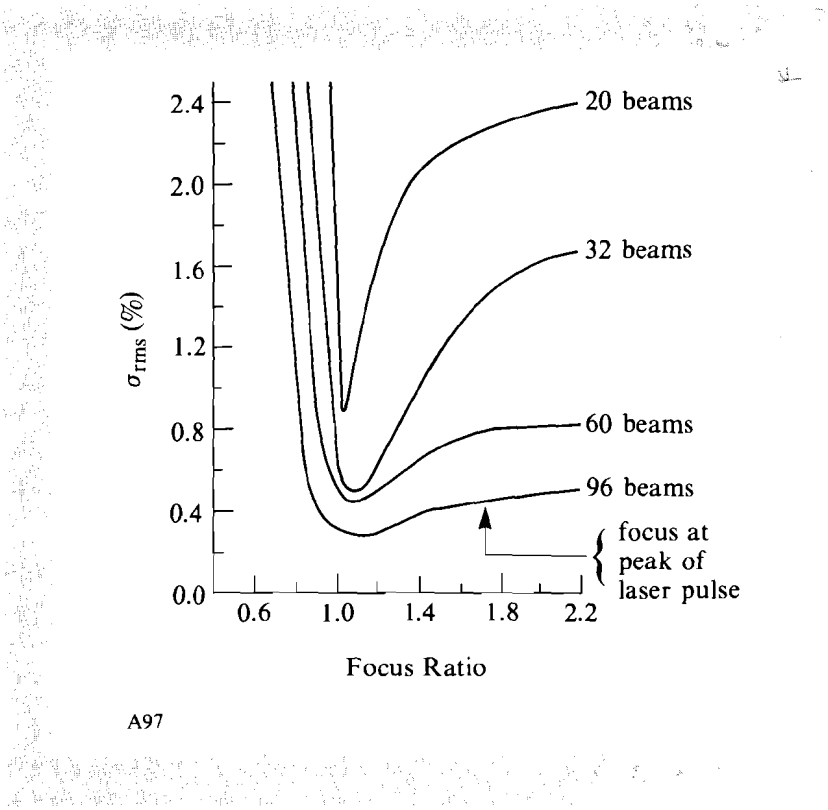

Fig. 38.3
Illumination uniformity as a function of focus position for 20-, 32-, 60-, and 96-beam geometries having 2% solid angle fraction.

uniformity throughout the pellet implosion. These simulations do not include the possible effects of thermal smoothing[23] of illumination nonuniformities in the pellet corona. While further experimental and theoretical understanding of the role of thermal smoothing would possibly allow for the use of less than 60 beams, when factors such as power imbalance and individual beam mispointing are included in the uniformity calculations, systems with substantially less than 60 beams fail to provide the necessary illumination uniformity over the duration of the implosion.

Since our laser system has a fixed number of beams, much of our research effort has been devoted to understanding, modifying, and controlling the single-beam factor.[4–7] Controlling power balance and the individual laser-beam profiles has shown great promise for future direct-drive implosions. Implementation of both a more stringent control of power balance and an initial form of beam smoothing [smoothing by spectral dispersion (SSD)[7]] has resulted in improved target performance for gas-fuel, glass-pusher experiments on OMEGA.

Understanding both the effects of illumination nonuniformity on pellet performance and how to reduce and control the level of illumination nonuniformity on target represents an extremely important physics issue for which more information is required. Our discussion of uniformity has been presented independent of a particular high-gain design. Simulations have shown that the required level of illumination uniformity is approximately the same for all high-gain designs in the energy range of 1.0 to 10.0 MJ.

Theoretical and experimental work is under way at LLE to continue to improve the single-beam factor associated with illumination uniformity on OMEGA. Based on our understanding of how to control power balance and improve individual beam profiles, the current OMEGA laser system does not provide adequate illumination uniformity to perform experiments that are hydrodynamically similar to that of a high-gain pellet.

Three key physics issues can best be presented by using a particular high-gain, direct-drive pellet design. As an example, we examine the single-shell, CH-ablator design shown schematically in Fig. 38.4(a). The applied laser pulse, shown in Fig. 38.4(b), is temporally shaped over ~45 ns and contains ~3.4 MJ of ultraviolet (351-nm) light. This pulse, shown in Fig. 38.4(b), has been optimized to maximize the overdense shell thickness, while maintaining a low-fuel isotrope, with minimum laser intensity on target. The calculated absorption efficiency (η_a) for this implosion is ~90%. The laser intensities at the quarter- and tenth-critical surfaces are shown in Fig. 38.4(c). These intensities represent the total intensity on target while the peak intensities for each individual beam would be $\sim 4 \times 10^{13}$ W/cm^2, well below the threshold for plasma instabilities.

Laser-light coupling and possible detrimental plasma physics effects during a direct-drive, high-gain implosion represent a second key physics issue for which little experimental data exists. Experimental and theoretical comparisons show that observables, such as the absorption efficiency, can be adequately modeled using inverse Bremsstrahlung and a ray-trace treatment. Current direct-drive implosion experiments are carried out on implosions that have extremely short-density scale lengths in comparison with high-gain designs. While a large number of theoretical simulations and calculations have been performed to estimate the effects of laser light transversing large-density scale lengths, little or no experimental data exists for density scale lengths/intensity regimes found in MJ-scale, high-gain capsule implosions. What experiments have been carried out on long-scale-length plasmas were done with laser-beam profiles that would not be adequate for high-gain, direct-drive. Extrapolating from these experiments could prove faulty because some of the observables may have been influenced by the poor quality of the laser beams used in the experiments.

The next key physics issue considered is hydrodynamic stability and its effect on high-gain pellet implosions. Figure 38.4(d) displays the in-flight aspect ratio as a function of time for the 3-MJ implosion. The in-flight aspect ratio can be considered to represent a measure of the target's ability to withstand shell breakup due to the Rayleigh-Taylor hydrodynamic instability . The in-flight aspect ratio is defined as $A(t) = R(t)/\Delta R(t)$, where $\Delta R(t)$ is found by first determining the radial location and value of the peak material density in the imploding pellet. The positions for density values of $1/e$ of the peak determine $\Delta R(t)$, and the average of these two locations is $R(t)$. This definition accounts for ~77% of the imploding shell mass, the cold fuel layer, and the pusher surrounding the central hot-spot region. Rayleigh-Taylor

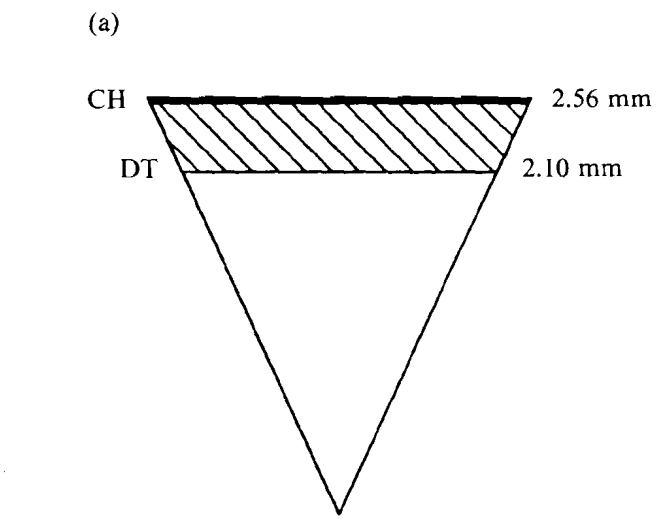

TC2455

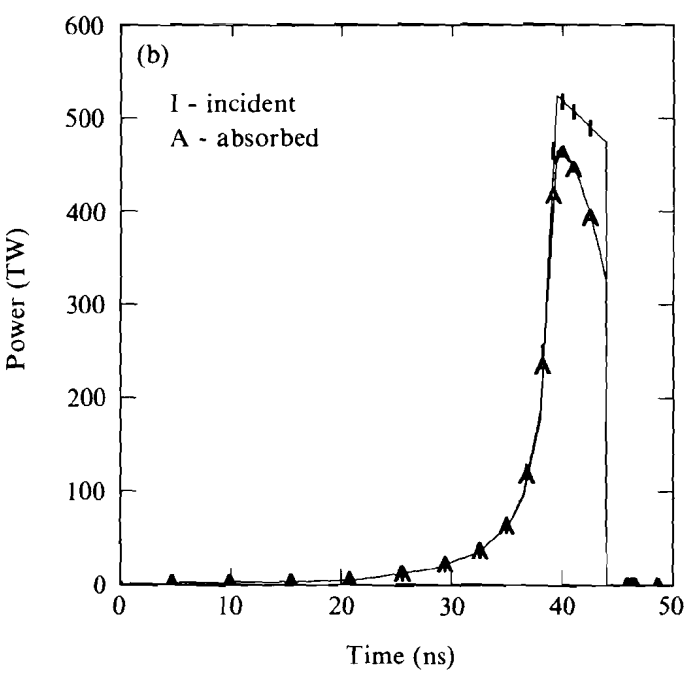

TC2464

Fig. 38.4
One-dimensional (*LILAC*) hydrodynamics simulation of a 3-MJ, 351-nm, single-shell, direct-drive, high-gain design.
(a) Schematic of pellet.
(b) Temporal pulse shape: *I*-incident, *A*- absorbed.
(c) Laser intensity at ¼ critical density (*Q*) and 1/10 critical density (*T*).
(d) In-flight aspect ratio and layer-radii in-flight aspect ratio (*A*).

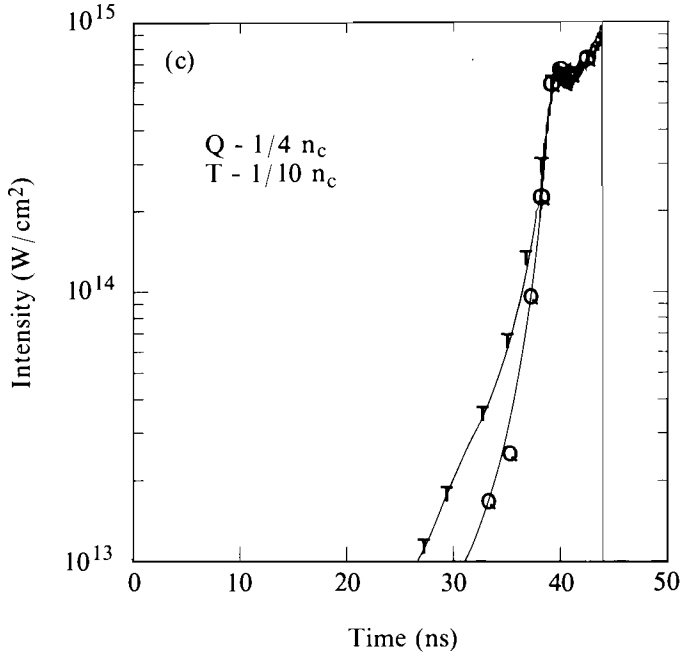

TC2459

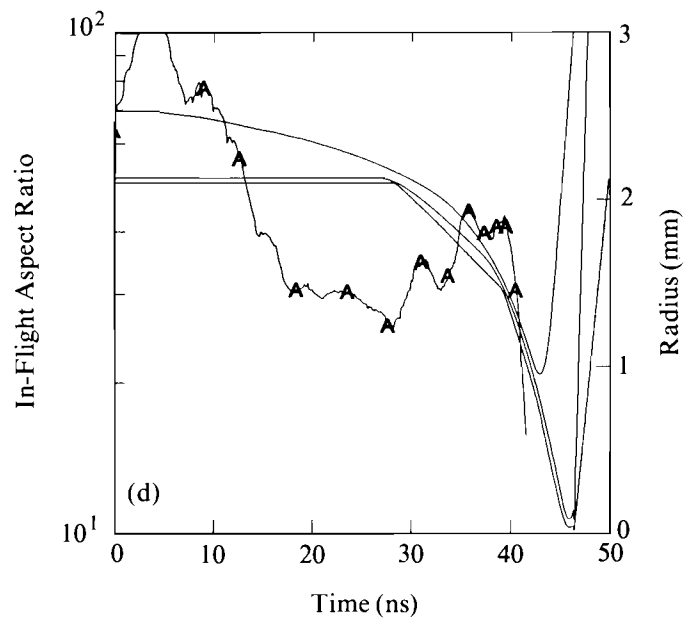

TC2476

unstable growth of this material into the main fuel mass during the acceleration and deceleration phases is important to determine pellet performance. [The algorithm used to determine $A(t)$ will pick up and follow shocks that are moving through the overdense fuel pellet during the acceleration phase. This results in what appears to be large values of the in-flight aspect ratio for short periods of time and can be seen in Fig. 38.4(d) as the spike-like structures at $t < 10$ ns when the "first" shock is moving through the pellet and again at 30, 35, and 40 ns.] The in-flight aspect ratio for this design peaks at ~ 40 during the time of maximum acceleration. A large number of theoretical calculations of the development and effects of the Rayleigh-Taylor instability on direct-drive pellet implosions[24–26] have, in general, found that the growth of the instability, in the presence of ablation, is reduced when compared to the classical value. Simulations have shown that the effects of the instability will, in general, depend on the growth and possible mode-mode interactions of all of the modes that are seeded (both by illumination nonuniformities and target imperfections) during the implosion.

Whether the present target design with a peak in-flight aspect ratio of 40 will survive the effect of Rayleigh-Taylor unstable growth during the acceleration phase will depend on the spectrum, initial amplitudes, and amplification of the seeded modes. At this time, these important factors can only be estimated theoretically. A limited number of important Rayleigh-Taylor experiments[27–29] have been carried out on direct-drive targets. However, due to the complexity of both the experiments and their interpretation, these represent a very limited set of data against which direct-drive simulations can be compared.

A final key issue for which no laboratory data currently exists is the physics associated with hot-spot formation and ignition of a direct-drive, high-gain design. At the culmination of the implosion, the imploding fuel material (all of the CH ablator has been ablated away by this time) is typically moving inward with a mass-averaged velocity of $\sim 3.0 \times 10^7$ cm/s. The shock energy, kinetic energy, and pressure-volume work associated with the imploding shell, balanced against radiative and conductive losses, are transformed into internal energy of the hot-spot material. For these designs the hot spot is composed of the initially gaseous material and a thin layer of material that was initially located at the very inner edge of the main fuel layer. Figure 38.5 schematically displays the conditions of the hot spot and main fuel layer at the time of ignition. In the hot spot, the ion temperature is usually between 5 keV and 10 keV with a density of ~ 60 g/cm^3. At these temperatures, densities, and fuel areal densities (ρR), the alpha particles from thermonuclear reactions begin to redeposit their energy in the hot spot. As this happens, the hot spot begins to self-heat, resulting in further fusion reactions, which deposit their energy in a region just outside of the hot spot, which results in the rapid heating of the surrounding fuel ("boot strapping"). Newly created alpha particles deposit their energy further out in the fuel while fuel layers adjacent to the hot spot begin to burn, producing more alpha particles and more heat. Thus, a thermonuclear burn wave propagates outward consuming the remaining fuel material. The fuel eventually disassembles as a

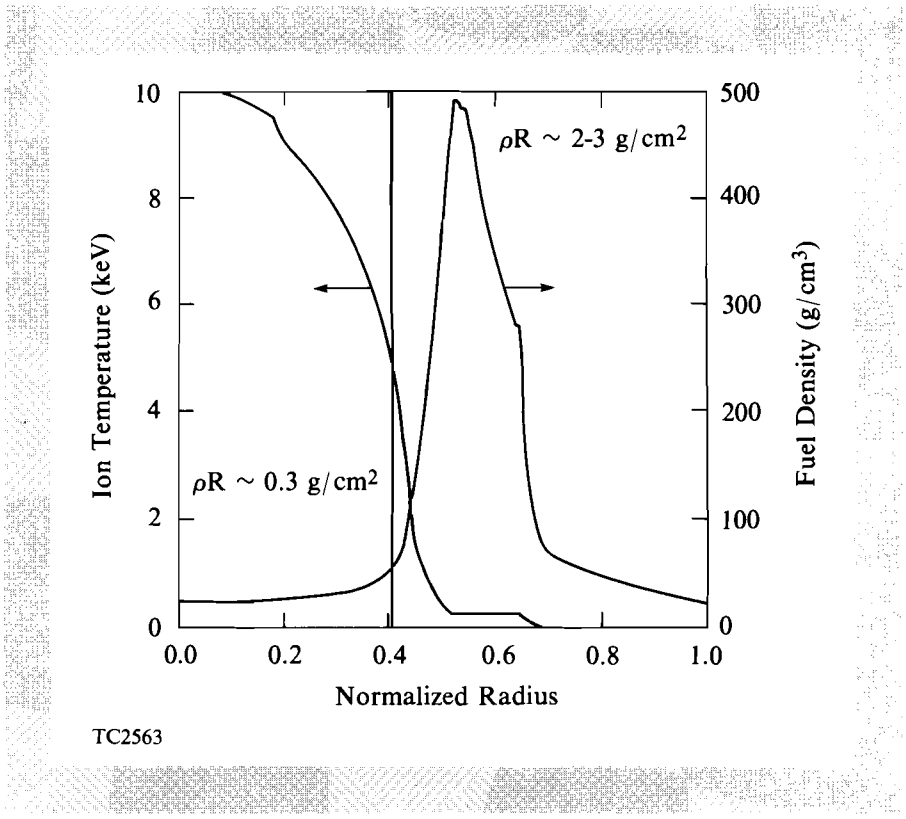

Fig. 38.5
Schematic of hot-spot region near time of ignition for high-gain pellet design composed of DT.

rarefaction wave propagates back through the fuel to the origin. Two-dimensional numerical simulations of these pellet designs (composed of only DT during the final stagnation phase) show that, if the spark plug ignites, the radially outward-propagating burn wave will result in essentially "1-D" yields even if the main fuel layer is moderately distorted.

Simulations have shown that the hot spot will fail to ignite if large perturbations are present during the formation of the spark plug.[17] The presence of long-wavelength perturbations ($\ell < 8$) can cause the internal energy of the fuel forming the hot spot to be converted into kinetic energy due to incoming, distorted, "cold" DT from the main fuel layer. Calculations indicate that the mixing of cold and hot DT, due to the Rayleigh-Taylor instability during the deceleration phase of implosion, can preclude ignition. Experimental data are required to increase understanding of important processes in hot-spot formation and ignition. This issue is tied to all of the three key physics issues we have discussed. Illumination nonuniformity can cause secular or Rayleigh-Taylor unstable growth, which can adversely affect pellet performance during the acceleration phase and subsequently the hot-spot formation during the deceleration phase. Any error in our understanding of the absorption of the laser light and, eventually, the energy available to the fuel will have important effects on the required

energy to drive a given high-gain pellet. The high-gain design presented in this section was carried out using our current "best" theoretical understanding of these key physics issues. It is clear, however, that until our understanding is confirmed by experiments, there will always be some question about the validity of such designs.

In order to obtain the experimental data base and theoretical understanding of the four key physics issues, any new direct-drive experimental facility will, in addition to carrying out well-diagnosed pellet implosions, have to be both a laser illumination uniformity and pulse-shaping "test bed." To estimate the amount of drive energy required by this system, if all four of the key physics issues presented previously are to be addressed, we first examine the issue of hot-spot physics/ignition scaling. The hot spot of a direct-drive, high-gain design is both hot (5 keV to 10 keV) and dense (~300 times liquid density). These conditions place constraints on the minimum energy of the system. Using the definition of ignition put forth by Nuckolls[30] [ignition is defined to occur when the liberated alpha-particle energy redeposited back into the fuel equals the energy invested to compress the fuel ($E_{\text{fuel}} \approx 1/5\ E_{\text{fusion}}$)], one can obtain an estimate of the required fuel temperature and areal density. This is shown in Fig. 38.6 where the hatched region represents the fuel ρR region between ~0.2 and 0.3 g/cm^2. The driver energy can then be estimated as a function of coupling efficiency ($\eta_c = \eta_a \eta_H$, where η_H is the hydrodynamic

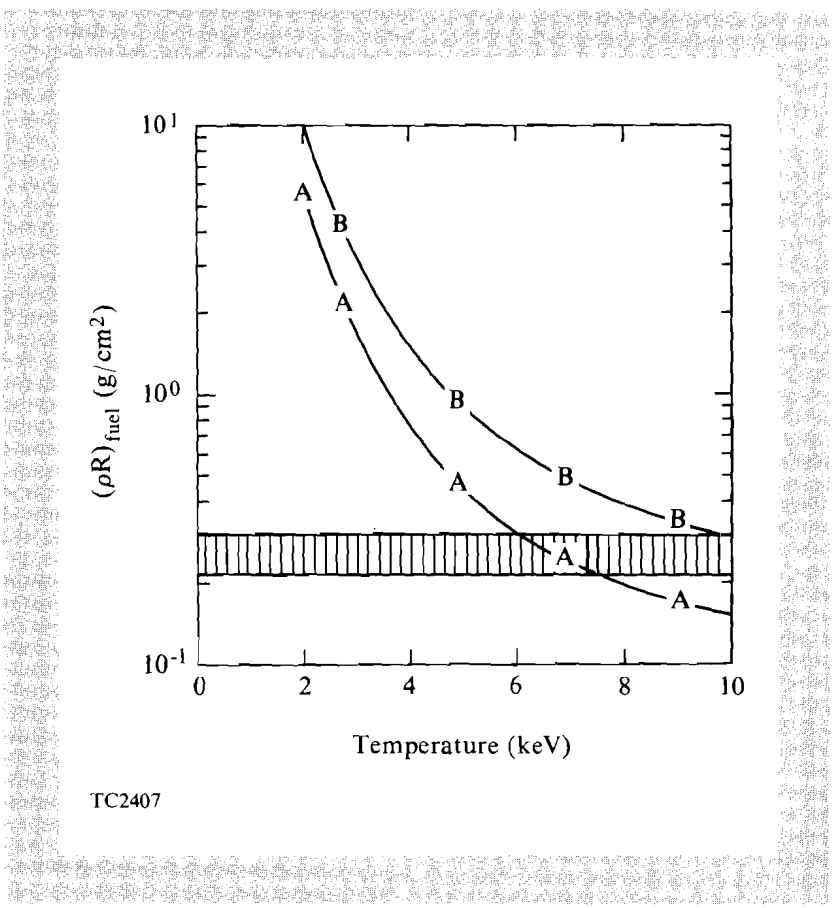

Fig. 38.6
Fuel areal density (ρR), temperature regime of ignition based on the definition in Ref. 30. *A*: confinement time given as R/C_s; *B*: confinement time given as $R/(2C_s)$.

efficiency) and compression for a given temperature, fuel ρR, and disassembly time multiplier [$E_{driven} \propto 1/\eta_c(\rho_{fuel})^2$]. As an example, the driver energy required for a fuel temperature of 7 keV and a disassembly time given by R/C_s (where R is the fuel radius and C_s is the sound speed) is shown in Fig. 38.7. For coupling efficiencies between that predicted for the 351-nm, high-gain, direct-drive designs presented in Sec. 1 and modest compressions, laser energies between 20 kJ and 100 kJ are required to meet the Nuckolls definition of ignition. (One could reduce the laser energy by increasing the compression; however, hydrodynamic-stability issues could place severe constraints on achieving such high compressions.) These simple estimates indicate that, in order to examine physics issues related to hot-spot formation and ignition, laser energies in excess of 20 kJ on target will be required.

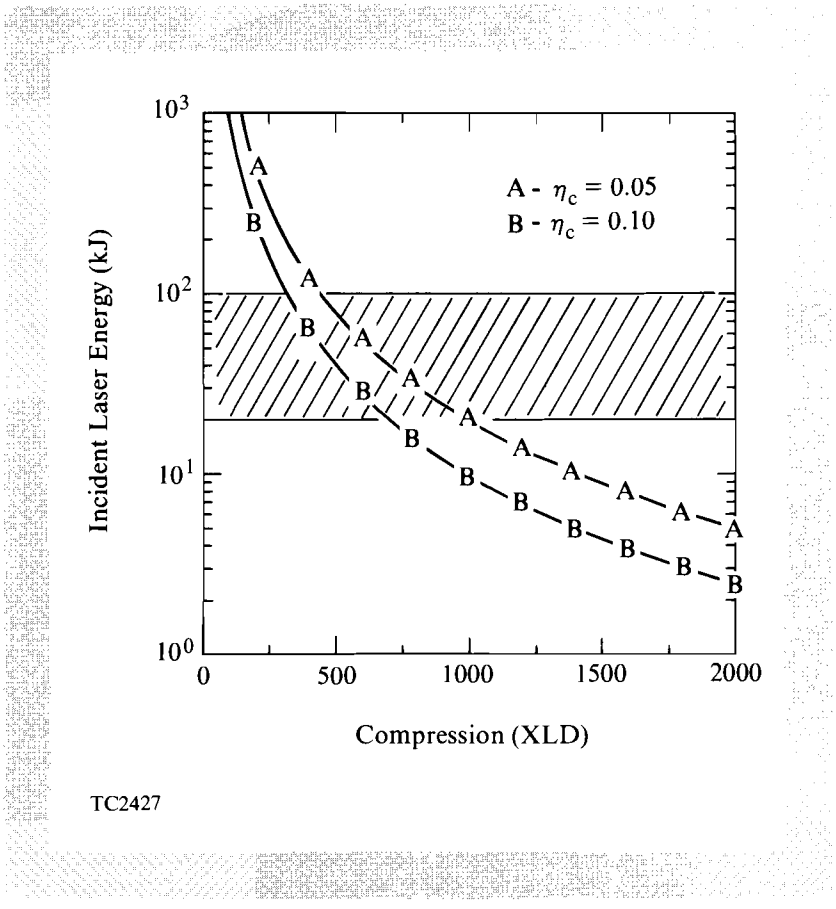

Fig. 38.7
Incident laser energy versus compression for ignition at a temperature of 5 keV and confinement time given by R/C_s. *A*: coupling efficiency (η_c) = 0.05; *B*: coupling efficiency = 0.10.

Having identified an energy threshold for this facility, one can then investigate hydrodynamically equivalent pellet designs, that is designs whose physical behavior scales to those appropriate for high gain. If a target is described by its hydrodynamic behavior alone, it can be scaled in size by the following relations:

Energy: $E \propto R^3$
Power: $P \propto R^2$
Time: $t \propto R$

This scaling, while not strictly valid because of changes associated with transport processes during implosion and thermonuclear reaction and transport processes during the burn phase, serves as a starting point for a 30-kJ, high-gain, hydrodynamic-equivalent design obtained by scaling the 3-MJ design presented in the previous section. The two pellets are shown in Fig. 38.8 (note sizes are not to scale). Similarly, the pulse shape shown in Fig. 38.4(b) was scaled down resulting in the curve labeled *S* in Fig. 38.9. One- and two-dimensional simulations show that this energy-scaled pellet design has a similar in-flight aspect ratio $\lesssim 40$, a hot-spot convergence ratio $\lesssim 25$, and the same uniformity requirements as the 3-MJ design. The solid, unlabeled curve in Fig. 38.9 represents a pulse consisting of two Gaussian pulses truncated at ~ 6.5 ns. This pulse shape, while not possessing all of the desired characteristics of the scaled pulse, has been shown numerically to be a good "initial" approximation to the pulse shape that the new facility should have.

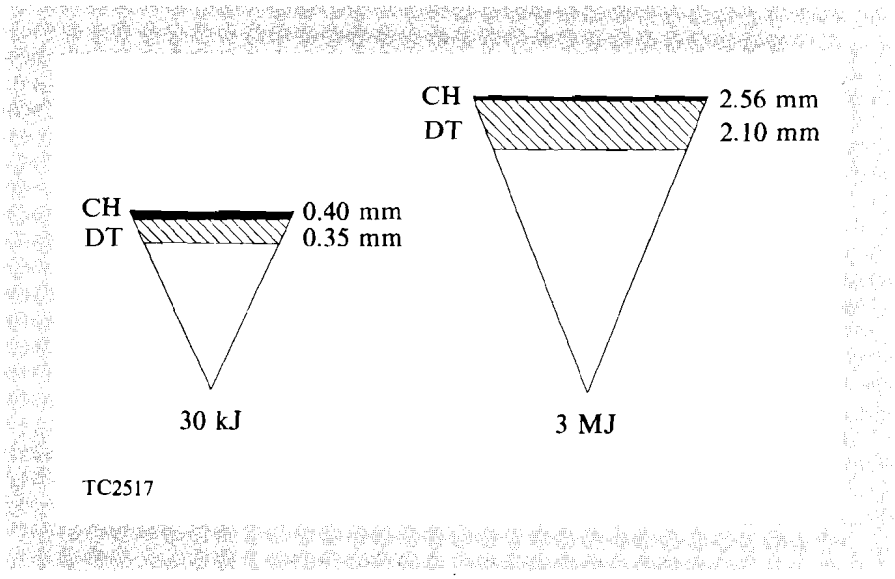

Fig. 38.8
Schematic of energy-scaled, 30-kJ, hydrodynamic-equivalent pellet design and initial 3-MJ pellet design. Note pellets are not drawn to scale.

Current theoretical work associated with SSD has shown that, with further modifications and the use of 60 beams, illumination nonuniformities could be reduced to the level required to do relevant hydrodynamic-equivalent experiments ($\sim 1\%$ to 2% σ_{rms}). The facility should be designed with enough flexibility to allow for changes to be made to the single-beam factor (principally the individual beam profiles) so that illumination-uniformity improvements could be incorporated as they become available.

The energy-coupling issues presented in the first section would have to be addressed in two parts. The energy-scaled target presented in Fig. 38.8 would not have a scale length as large as that of the high-gain design. However, the experimental data associated with energy coupling obtained on the hydrodynamic-equivalent targets (which have

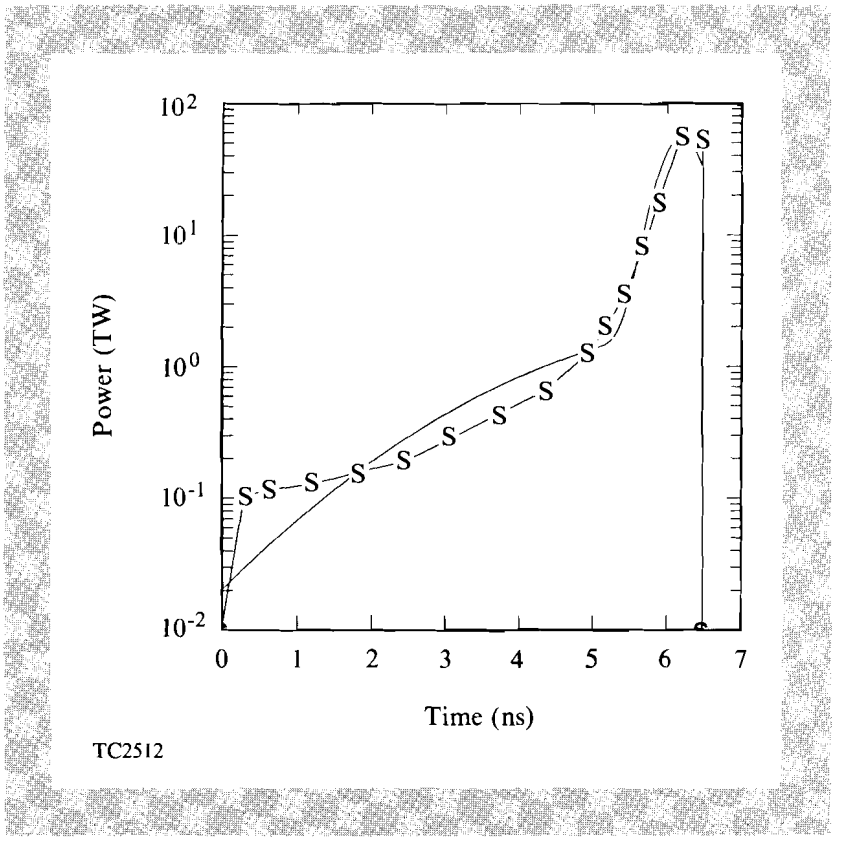

Fig. 38.9
Energy-scaled pulse shapes. *S* represents the scaled 3-MJ pulse shape; the solid curve represents a pulse shape constructed of two truncated Gaussian pulses, which could serve as the initial pulse shape the system could produce.

density scale lengths larger than those of present direct-drive experiments) would serve as an additional check of our understanding of how laser light couples to the target. Issues more relevant to the density scale length/intensity regime associated with high-gain designs could also be addressed using flat targets and a limited number of laser beams, similar to techniques successfully used on NOVA.[31] Such experiments could generate long-scale-length plasmas using individual laser beams more characteristic of those of high-gain, direct-drive implosions.

We believe that a 30-kJ, 351-nm, 60-beam laser system can provide the necessary experimental data base required to determine the role of direct-drive in future ICF planning. While the issues presented in this article were limited to direct drive, it is evident that the data base obtained from such a facility would also prove important in understanding processes associated with high-gain, indirect-drive pellet implosions. Subsequent articles in this and the next LLE Review will discuss in more detail the design of the OMEGA upgrade.

ACKNOWLEDGMENT

This work was supported by the U.S. Department of Energy Office of Inertial Fusion under agreement No. DE-FC03-85DP40200 and by the Laser Fusion Feasibility Project at the Laboratory for Laser Energetics, which has the following sponsors: Empire State Electric Energy Research Corporation, New York State Energy Research and Development Authority, Ontario Hydro, and the University of Rochester. Such support does not imply endorsement of the content by any of the above parties.

REFERENCES

1. J. H. Nuckolls, *Phys. Today* **35**, 24 (1982).
2. R. L. McCrory, J. M. Soures, C. P. Verdon, F. J. Marshall, S. A. Letzring, S. Skupsky, T. J. Kessler, R. L. Kremens, J. P. Knauer, H. Kim, J. Delettrez, R. L. Keck, and D. K. Bradley, *Nature* **335**, 225 (1988).
3. LLE Review **35**, 97 (1988).
4. R. H. Lehmberg and S. P. Obenschain, *Opt. Commun.* **46**, 27 (1983).
5. Y. Kato *et al.*, *Phys. Rev. Lett.* **53**, 1057 (1984).
6. LLE Review **33**, 1 (1987).
7. LLE Review **37**, 29 (1989).
8. R. A. Sacks and D. H. Darling, *Nucl. Fusion* **27**, 447 (1987).
9. B. I. Bennett, J. D. Johnson, G. I. Kerley, and G. T. Rood, Los Alamos National Laboratory Report LA-7130 (1978).
10. W. F. Huebner, A. L. Merts, N. H. Magee, and M. F. Argo, Los Alamos National Laboratory Report LA-6760-M (1977).
11. M. Born and E. Wolf, *Principles of Optics* (Pergamon, New York, 1975), p. 123.
12. R. C. Malone, R. L. McCrory, and R. L. Morse, *Phys. Rev. Lett.* **34**, 721 (1975).
13. C. P. Verdon, F. J. Marshall, S. Letzring, D. K. Bradley, J. Delettrez, R. L. Keck, J. P. Knauer, R. L. Kremens, R. L. McCrory, S. Skupsky, and J. M. Soures, *Bull. Am. Phys. Soc.* **33**, 2006 (1988).
14. G. J. Taylor, *Proc. R. Soc. London, Ser. A* **201**, 192 (1950).
15. D. J. Lewis, *Proc. R. Soc. London, Ser. A* **202**, 81 (1950).
16. S. Chandraeskhar, *Hydrodynamic and Hydromagnetic Stability* (Clarendon Press, Oxford, England, 1961), Chap. 10.
17. LLE Review **23**, 125 (1985).
18. Lawrence Livermore Laboratory Laser Program Annual Report UCRL-50021-74, p. 219 (1975).
19. J. Howard, *Appl. Opt.* **16**, 2764 (1977).
20. A. J. Scannapieco and H. Brysk, *J. Appl. Phys.* **50**, 5142 (1979).
21. K. Lee, R. L. McCrory, and R. Hopkins, Laboratory for Laser Energetics Report No. 88 (1981).
22. S. Skupsky and K. Lee, *J. Appl. Phys.* **54**, 3662 (1983).
23. S. E. Bodner, *J. Fusion Energy* **1**, 221 (1981).
24. M. H. Emery, J. H. Gardner, and J. P. Boris, *Phys. Rev. Lett.* **48**, 677 (1982).